Scanning Tunneling Spectroscopy of One-Dimensional Surface States on a Metal Surface

A. Biedermann,[1] O. Genser,[1] W. Hebenstreit,[1] M. Schmid,[1] J. Redinger,[2] R. Podloucky,[3] and P. Varga[1,*]

[1]*Institut für Allgemeine Physik, Technische Universität Wien, A-1040 Vienna, Austria*
[2]*Institut für Technische Elektrochemie, Technische Universität Wien, A-1060 Vienna, Austria*
[3]*Institut für Physikalische Chemie, Universität Wien, A-1090 Vienna, Austria*

(Received 2 January 1996)

Scanning tunneling spectroscopy permits real-space observation of one-dimensional electronic states on a Fe(100) surface alloyed with Si. These states are localized along chains of Fe atoms in domain boundaries of the Fe(100) $c(2 \times 2)$Si surface alloy, as confirmed by first-principles spin-polarized calculations. The calculated charge densities illustrate the *d*-like orbital character of the one-dimensional state and show its relationship to a two-dimensional state existing on the pure Fe(100) surface. [S0031-9007(96)00335-3]

PACS numbers: 61.16.Ch, 71.15.Mb, 71.20.Be, 73.20.Dx

The electronic properties of alloy surfaces are of importance for several surface and interface related applications like metal-metal or semiconductor-metal heteroepitaxy and heterogeneous catalysis. Scanning tunneling microscopy and spectroscopy (STM and STS) provides the possibility to study directly the electronic structure of *disordered alloy* surfaces. The combination with first principles calculations permits the detailed analysis of novel electronic features due to alloying of the pure metal surface. Moreover, the comparison of the STM images to the calculated charge densities can help one to find an answer to the key question for the reasons of the chemical contrast observed on metal alloy surfaces [1].

Free-electron-like surface states existing on many noble metal surfaces are known to influence strongly the adsorption characteristics of these surfaces [2]. They give rise to a variety of corrugation patterns in the STM images due to quantum interference of surface electrons scattered at defects or steps [3,4]. Tunneling into such element specific surface states [5] or image states [6] in principle provides a simple means of chemical selectivity. The delocalized nature of these surface states, however, does not permit chemical resolution on an atomic scale.

In this Letter we present images and tunneling spectra of surface states on the pure and Si-covered Fe(100) surface. First principles calculations show that the Fe surface states are essentially *d*-like and much more localized at the atomic sites than the *sp*-like states on noble metal surfaces. On alloying the pure Fe surface with Si these surface states are not completely quenched. Their wave functions still show high amplitude along chains of iron atoms in domain boundaries of the ordered Si/Fe(100) surface alloy, but low amplitude near the Si atoms. This results in a strong image contrast between the Fe-rich domain boundaries and the Si-covered domains.

One-dimensional surface states have been proposed for reconstructed [7], adsorbate covered [8], and stepped [9] metal surfaces on the basis of (inverse) photoelectron spectroscopy. These methods, however, lack spatial resolution and thus only indirectly infer the one-dimensional character of certain electronic states from experimental evidence.

The full-potential linearized augmented plane wave (FLAPW) method [10,11] adapted for thin films is used to calculate the electronic structure of a 9 layer Fe(100) and a 7 layer Si/Fe(100) slab. The result is presented in the form of local densities of states (LDOS), decomposing the total DOS into contributions from individual atomic spheres around the constituting Fe and Si cores, from the interstitial region between them, and the vacuum region. For comparison with the STM spectra the vacuum LDOS itself is calculated for ten slices parallel to the surface and up to 1 nm above.

An ideal bulk truncation for the slabs was used since the pure Fe(100) surface exhibits only a very small inward relaxation (-1.5% [12]). Moreover, the exact Si positions should be of minor relevance since the wave functions of the investigated kind of surface states show only very low probability density near the Si atoms.

STM and STS measurements were performed in ultrahigh vacuum (UHV) using a commercial STM (Omikron μ-STM) operated with an electrochemically etched W tip. The tip was sputter cleaned in UHV and frequently conditioned by voltage pulses during tunneling. The Fe(100) and $Fe_{96.5}Si_{3.5}$(100) single crystal samples were cleaned by sputtering with 1 keV Ar^+ ions. Surfaces with (10–40)% Si coverage were prepared by heating the Si-alloyed sample for 2–10 min to 750 K. It is known from previous experiments that Si atoms diffuse during annealing from the bulk to the surface, where they substitute surface Fe atoms and form an ordered Fe(100) $c(2 \times 2)$Si surface alloy [13]. Already in the second monolayer the Si concentration is expected to be close to the bulk concentration.

Based on the Tersoff-Hamann theory [14] it can be argued that for low tunneling voltages [15] the tunneling conductance spectrum dI/dV (tunneling current I, voltage V) should be approximately proportional to the energy dependent LDOS just at the center of the tunneling tip. Figure 1 compares the calculated LDOS at 1 nm above the pure Fe(100) surface with an averaged

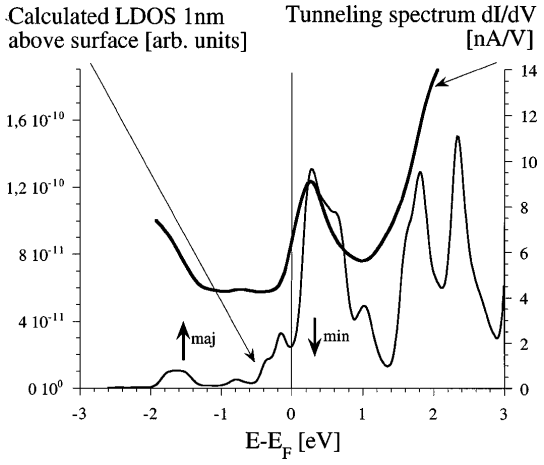

FIG. 1. The two-dimensional surface state on Fe(100): Tunneling spectrum averaged over independent measurements and image points (tip-sample distance adjusted at $V_{\text{sample}} = -1$ V and $I = 1$ nA) and spin-integrated FLAPW-LDOS 1 nm above the surface (smoothed with Gaussian 0.2 eV FWHM). The arrows mark the positions of the corresponding exchange-split minority-spin and majority-spin components of the surface resonance band in discussion.

tunneling spectrum proving good agreement between theory and experiment concerning the intense peak 0.3 eV above the Fermi energy. At higher tunneling voltages the spectrum is superimposed on an exponentially increasing background, which makes a useful evaluation rather difficult. From I/z measurements we estimate a value for the tip-sample distance z of about 0.8 nm for an experimental tunneling resistance of 1 GΩ.

The states causing the peak just above the Fermi edge can easily be traced back to their locations in the minority spin band structure. They belong to a resonance band around the center of the surface Brillouin zone and contribute most to the LDOS in the vacuum region at 1 nm above the surface. Although the resonance band shows considerable (upwards) dispersion, the states near $\bar{\Gamma}$ dominate the vacuum region leading to a rather narrow peak in the tunneling spectrum 0.3 eV above the Fermi edge. The majority component causes a much smaller peak in the LDOS due to the larger vacuum barrier and hence faster decaying vacuum tails and might be detectable only at smaller tip-sample distances.

On approaching the $\bar{\Gamma}$ point the resonance becomes more and more surface localized until it ends up as a true surface state at the center of the Brillouin zone where a $\bar{\Gamma}_1$ symmetry gap exists [16]. Its charge density is displayed in Fig. 2 and clearly shows $d_{3z^2-r^2}$ character. The *sp* admixture to this surface state shows up in both a strong asymmetry with respect to the surface plane and a lateral delocalization in the vacuum region. It seems plausible that it is just this delocalization and interaction of neighboring atoms which makes the state so easily visible for the STM.

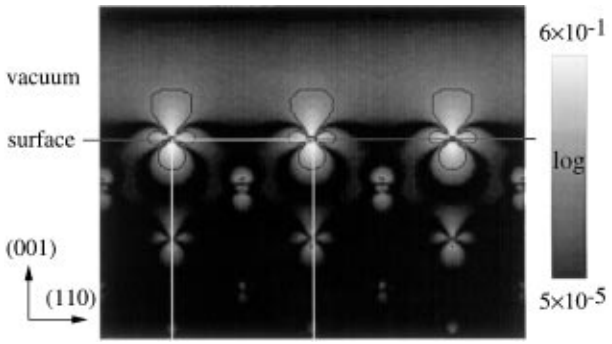

FIG. 2. The charge density distribution of the Fe(100) $\bar{\Gamma}_1$ surface state responsible for the peak in the STS spectra 0.3 eV above the Fermi edge. The rectangle outlined in white marks the upper half of the unit cell with two surface atoms at its corners. The constant density contour illustrates the $d_{3z^2-r^2}$ orbital character.

This $\bar{\Gamma}_1$ surface state already was found in an early non-self-consistent calculation [16,17] and its correct band energy was obtained by a later self-consistent spin-polarized calculation [18]. Similar states exist also on other bcc (100) surfaces near the Fermi edge, for instance, on W(100) (-0.3 eV) [19] and Mo(100) (-0.2 eV) [20]. Almost simultaneously to our work the existence of such states has been confirmed by tunneling spectroscopy on Fe(100) and Cr(100) by Stroscio *et al.* [21].

Surprisingly also the annealed surface of an $Fe_{96.5}Si_{3.5}(100)$ single crystal, covered with about 35% Si, shows a surface state peak in laterally averaged tunneling spectra. The peak position, however, is shifted from 0.3 eV above the Fermi edge to 0.6 eV. In striking contrast, on an Fe(100) surface covered with 20% oxygen the surface state is completely quenched.

Scanning tunneling spectroscopy permits direct imaging of the spatial charge distribution of the surface states corresponding to the peak in the spectra 0.6 eV above the Fermi edge. In the present case it is sufficient to image at positive sample voltages, for which the current is strongly influenced by the surface state charge density due to tunneling from the tip into unoccupied surface states. The resulting STM image is displayed in Fig. 3. The surface state is localized along linear structures which turn out to be antiphase domain boundaries of the ordered $c(2 \times 2)$Si superstructure and consist of zigzag Fe chains [Fig. 3(b)]. These domain boundaries show up as bright bands between laterally displaced $c(2 \times 2)$Si patterns (see white line in Fig. 3). Within the $c(2 \times 2)$Si regions, appearing darker [Fig. 3(c)], the spectra do not show any features.

The domain structure is a consequence of the rather low heating temperature of 750 K which does not allow for an effective annealing of the surface. Heating to higher temperatures diminishes the domain boundary density and thereby the surface state peak in the spectra.

Small Fe islands which form due to one or two missing Si atoms representing a wider confinement structure than

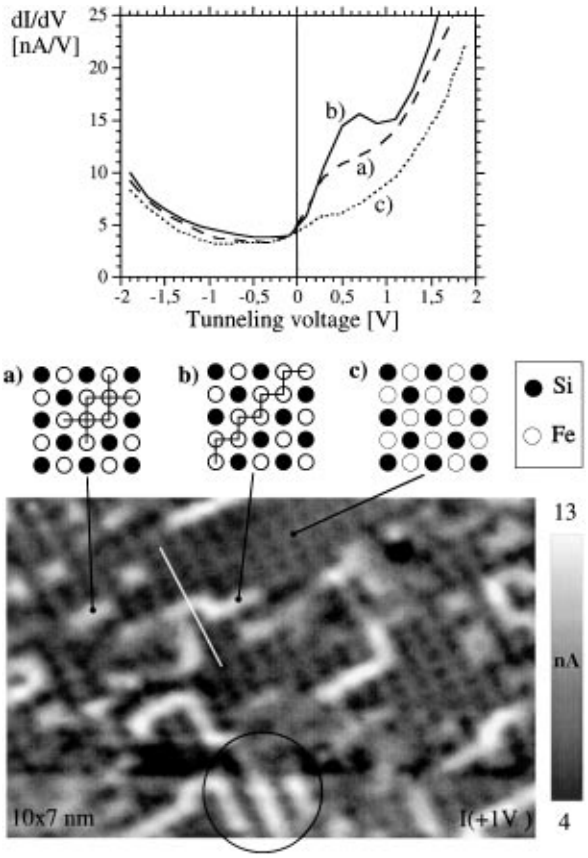

FIG. 3. STM image and tunneling spectra of characteristic regions of the $Fe_{96.5}Si_{3.5}(100)$ surface covered with about 35% Si. The STM image represents the current values at $V_{\text{sample}} = +1$ V. The tip sample distance was adjusted at $V_{\text{sample}} = -0.25$ V and $I = 1$ nA. (a) Fe island due to two missing Si atoms. (b) Domain boundary appearing as bright band in the image due to a one-dimensional surface state about 0.6 eV above the Fermi edge. The circle marks a small area with closely neighbored boundaries similar to the model structure used for the calculation. (c) Perfect $c(2 \times 2)$Si.

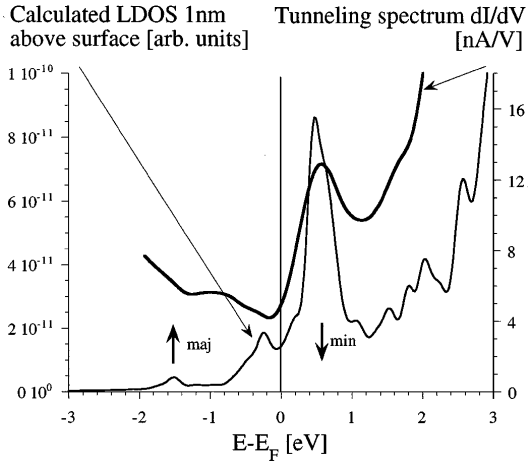

FIG. 4. The one-dimensional chain state on Si/Fe(100): Averaged tunneling spectrum above domain boundaries of the Fe(100) $c(2 \times 2)$Si superstructure and spin-integrated FLAPW-LDOS 1 nm above the surface (smoothed with Gaussian 0.2 eV FWHM). The peak 0.6 eV above the Fermi edge is caused by one-dimensional states along the Fe chains in the domain boundaries.

the domain boundaries do not show comparably intense surface state features [Fig. 3(a)]. This suggests that on increasing confinement the two-dimensional state is quenched before the chain state appears, demonstrating its intrinsically one-dimensional character.

To understand the nature of these states and their relation to the two-dimensional surface state of pure Fe(100), the electronic structure of a model surface geometry consisting of periodically repeated closely neighbored domain boundaries was calculated [Fig. 5(b)]. Such a periodic arrangement is also visible in certain areas of the STM image (Fig. 3, circle) and yields the same spectrum as the isolated boundaries. A comparison of the tunneling spectra with the calculated LDOS at 1 nm above the surface shows that the energy shift of 0.3 eV induced by the one-dimensional localization is correctly reproduced by the calculation (Fig. 4).

The charge density distribution of the corresponding $\bar{\Gamma}$ state parallel to the surface demonstrates the high degree of localization along the "zigzag" chains of Fe atoms [Fig. 5(b)]. The vertical section in Fig. 5(c) shows the modification of the orbital character that occurs on localization. The original $d_{3z^2-r^2}$ orbitals are strongly tilted, apparently to optimize the coupling of the charge lobes protruding from the surface [Fig. 5(a)]. Its surface state character is immediately clear by noting that more than 50% of the charge density is found near the surface Fe atoms and the vacuum region.

The seven layer slab, however, is too thin to decouple both surfaces of the slab perfectly, resulting in an energy split of about 50 meV. The coupling of neighboring chain states via the Fe atoms in the subsurface layers splits the surface state peak by another 150 meV, which indicates a rather weak interaction between neighboring chain states. Because of these weak couplings, the structural model applied by the calculation is well suited to describe the claimed localization effect.

For disordered surface alloys with low Si concentration the localization effect becomes even more important. According to our experimental observations as few as three Si atoms forming a very short domain boundarylike arrangement already induce one-dimensional localization. This accounts for an energy-shifted surface state peak in the tunneling spectra on significant fractions of a 10% Si covered surface. The one-dimensional coupling of the surface Fe atoms is enhanced by short range order of the Si atoms, i.e., the formation of Si pairs and chains.

In summary, we show that the $d_{3z^2-r^2}$-like surface states, which exist on pure Fe(100), transform into one-dimensional chain states along Fe-rich domain boundaries on a Si/Fe(100) surface alloy. Such a one-dimensional localization of the two-dimensional Fe surface state

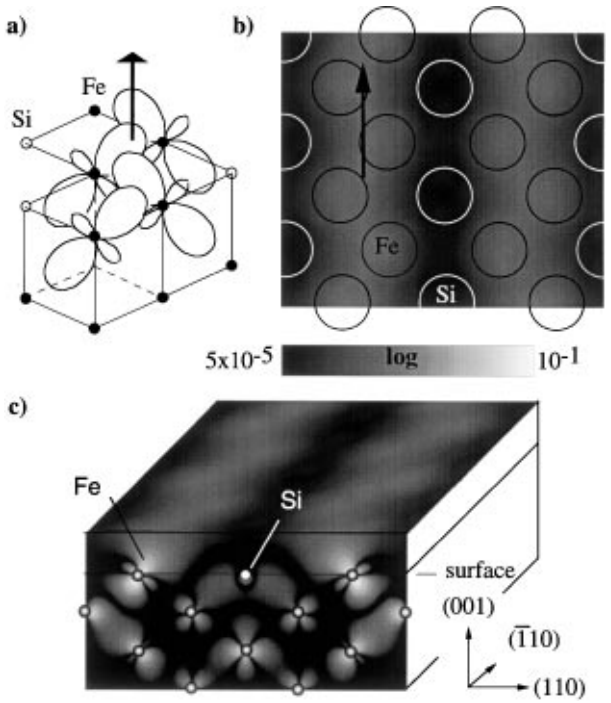

FIG. 5. One-dimensional $\bar{\Gamma}$ surface state along Fe zigzag chains separated by Si chains (periodic domain boundary structure). (a) Model of the "tilted" $d_{3z^2-r^2}$-orbital chain. (b) Charge density parallel to the surface and 0.15 nm above. (c) Pseudo-3D representation of the charge density distribution. Only the upper half of the symmetric 7 layer film is displayed.

occurs to some extent even on disordered Si/Fe(100) surface alloys, representing a mechanism for the persistence of surface states on disordered alloy surfaces. Equivalent two-dimensional surface states are known to exist also on several other bcc (100) surfaces where similar one-dimensional localization effects should be observable as well. Since alloy surfaces are often used in catalytic processes this phenomenon might be also relevant to mechanisms of enhanced catalytic activity or selectivity of transition metal alloys. Moreover, the weak interaction of Si and Fe via the surface state might be of interest for the possible use of two-dimensional Fe-Si structures as interlayers in magnetic metal superlattices.

The authors would like to thank P. Lejcek and K. D. Rendulic for the crystals. This work was supported by the "Fonds zur Förderung der Wissenschaftlichen Forschung" (Austrian Science Foundation) under Projects No. S6201-PHY and No. S6204-PHY, and the Center for Computational Materials Science, Vienna, Austria. R. P. gratefully acknowledges support by the Hochschuljubiläumsstiftung of the City of Vienna and by the HCM Ψ_k Network program.

*Electronic address: varga@iap.tuwien.ac.at

[1] M. Schmid, H. Stadler, and P. Varga, Phys. Rev. Lett. **70**, 1441 (1993).
[2] E. Bertel, P. Roos, and J. Lehmann, Phys. Rev. B **52**, 14 384 (1995).
[3] M. F. Crommie, C. P. Lutz, and D. M. Eigler, Nature (London) **363**, 524 (1993).
[4] Ph. Avouris and I.-W. Lyo, Science **264**, 942 (1994).
[5] Y. W. Mo and F. J. Himpsel, Phys. Rev. B **50**, 7868 (1994).
[6] T. Jung, Y. W. Mo, and F. J. Himpsel, Phys. Rev. Lett. **74**, 7868 (1994).
[7] E. Bertel and U. Bischler, Surf. Sci. **307–309**, 947 (1994).
[8] C. Binns, C. Norris, and M.-G. Barthes-Labrousse, Phys. Scr. **T45**, 283 (1992).
[9] J. E. Ortega, F. J. Himpsel, R. Haight, and D. R. Peale, Phys. Rev. B **49**, 13 859 (1994).
[10] E. Wimmer, H. Krakauer, M. Weinert, and A. J. Freeman, Phys. Rev. B **24**, 864 (1981).
[11] E. Wimmer, H. Krakauer, and A. J. Freeman, Adv. Electron. Electron Phys. **65**, 357 (1985).
[12] F. Jona, Surf. Sci. **68**, 204 (1977).
[13] A. Biedermann, M. Schmid, B. M. Reichl, and P. Varga, Fresenius J. Anal. Chem. **353**, 259 (1995).
[14] J. Tersoff and D. R. Hamann, Phys. Rev. B **31**, 805 (1985).
[15] G. Hörmandinger, Phys. Rev. B **49**, 13 897 (1994).
[16] E. Caruthers and L. Kleinman, Phys. Rev. Lett. **35**, 738 (1975).
[17] E. Caruthers, D. G. Dempsey, and L. Kleinman, Phys. Rev. B **14**, 288 (1976).
[18] C. S. Wang and A. J. Freeman, Phys. Rev. B **24**, 4364 (1981).
[19] M. Posternak, H. Krakauer, A. J. Freeman, and D. D. Koelling, Phys. Rev. B **21**, 5601 (1980).
[20] G. P. Kerker, K. M. Ho, and M. L. Cohen, Phys. Rev. B **18**, 5473 (1978).
[21] J. A. Stroscio, D. T. Pierce, A. Davies, R. J. Celotta, and M. Weinert, Phys. Rev. Lett. **75**, 2960 (1995).